

A Highly Effective and Robust Membrane Potential Driven Supervised Learning Method for Spiking Neurons

Malu Zhang, Hong Qu, *Member, IEEE*, Ammar Belatreche, *Member, IEEE*, Yi Chen, Zhang Yi, *Fellow, IEEE*

Abstract—Spiking neurons are becoming increasingly popular owing to their biological plausibility and promising computational properties. Unlike traditional rate-based neural models, spiking neurons encode information in the temporal patterns of the transmitted spike trains, which makes them more suitable for processing spatio-temporal information. One of the fundamental computations of spiking neurons is to transform streams of input spike trains into precisely timed firing activity. However, the existing learning methods used to realise such computation result in relatively low accuracy performance and poor robustness to noise. In order to address these limitations, we propose a novel highly effective and robust MEMbrane POTential driven supervised LEARNing method (MemPo-Learn), which is able to generate desired spike trains with higher precision, higher efficiency and better noise robustness than current state-of-the-art spiking neuron learning methods. While traditional spike-driven learning methods use an error function based on the difference between the actual and desired output spike trains, the proposed MemPo-Learn method employs an error function based on the difference between the output neuron membrane potential and its firing threshold. The efficiency of the proposed learning method is further improved through the introduction of an adaptive strategy, called Skip Scan Training Strategy (SSTS), that selectively identify the time steps when to apply weight adjustment. The proposed strategy enables the MemPo-Learn method to effectively and efficiently learn the desired output spike train even when much smaller time steps are used. In addition, we improve the learning rule of MemPo-Learn to help mitigate the impact of the input noise on the timing accuracy and reliability of the neuron firing dynamics. The proposed learning method is thoroughly evaluated on synthetic data and is further demonstrated on real world classification tasks. Performance comparisons against competitive learning methods for spiking neurons and state-of-the-art rate-based neural networks are presented. Experimental results show that the proposed method can achieve high learning accuracy with a significant improvement in learning time and better robustness to different types of noise.

Index Terms—Spiking neurons, supervised learning, spiking neural networks, membrane potential, gradient descent, classification.

This work was supported in part by the National Science Foundation of China under Grants 61573081, 61370073 and the Foundation for Youth Science and Technology Innovation Research Team of Sichuan Province 2016TD0018, and the Fundamental Research Funds for Central Universities under Grant ZYGX2015J062, and the China Postdoctoral Science Foundation 2017M612948.

M. Zhang, H. Qu and Y. Chen are with School of Computer Science and Engineering, University of Electronic Science and Technology of China, Chengdu 610054, P. R. China (e-mail: maluzhang@126.com; hongqu@uestc.edu.cn).

A. Belatreche is with Department of Computer and Information Science, Faculty of Engineering and Environment, Northumbria University, UK (e-mail: ammar.belatreche@northumbria.ac.uk).

Z. Yi is with College of Computer Science, Sichuan University, Chengdu 610065, China (e-mail: zhangyi@scu.edu.cn).

I. INTRODUCTION

Traditional rate coded artificial neural networks encode information through the firing rate of their biological counterparts. Although rate coding is commonly used in artificial neural networks, it is unlikely that rate-based coding can convey all the information related to rapid processing of visual scenes, odor, and sound [1]-[4]. As precise spike-timing neural activities have been observed in many brain regions, including the retina [5]-[7], the lateral geniculate nucleus [8] and the visual cortex [9], the view that information is represented by explicit timing of spikes rather than mean firing rate has received increasing attention [10], [11]. These findings have led to a new way of simulating neural networks based on spiking neurons which encode information by the firing times of spikes [12]-[14]. Theoretical analysis indicates that networks of spiking neurons can arbitrarily approximate any continuous function [15]. Furthermore, it has been demonstrated that networks of spiking neurons are computationally more powerful than traditional rate-based neurons [15]-[20]. However, their application to real world problems remain relatively limited due to the computational complexity of spiking neural networks and the lack of effective and efficient learning methods. Therefore the development of highly effective and robust learning methods is more important than ever to leverage the computational power of these biologically plausible neural networks and to increase their applicability in solving real world problems.

Supervised learning was proposed as a successful concept of information processing in traditional neural networks. The most documented evidence for supervised learning in the central nervous system (CNS) comes from the studies on the cerebellum and the cerebellar cortex [21], [22]. However, the exact mechanisms underlying supervised learning in the biological neurons remain an open problem [23], [24]. In order to train the spiking neurons to generate desired sequences of spikes, many supervised learning algorithms have been proposed. They can be broadly classified into two groups: spike-driven methods and membrane potential-driven methods.

Spike-driven methods use the desired and actual output spikes as the relevant signals for controlling synaptic change. Typical examples of these methods include SpikeProp [25] and the multispike learning algorithm [26] which construct an error function using the difference between the desired and actual output spikes, then use its gradient to update the synaptic connection weights. ReSuMe [23] is another spike-

driven method, in which synaptic weight changes are driven by the joint effect of two opposite processes: 1) strengthening of the synaptic weights through STDP based on the input and the desired output spike trains, and 2) weakening of the synaptic weights through anti-STDP based on the input and the actual output spike trains. To enhance the learning performance of ReSuMe, DL-ReSuMe [24] has recently been proposed to integrate the delay shift approach with ReSuMe-based weight adjustment. Both the Chronotron E-learning rule [27] and the SPAN learning rule [28] try to minimize the distance between the desired and actual output spike trains. The distance in the Chronotron E-learning rule is defined by the Victor and Purpura (VP) metric [29], while in the case of the SPAN rule the distance is based on a metric similar to the van Rossum metric [30]. Common disadvantages of the above mentioned methods include relatively low learning efficiency and accuracy.

In an attempt to improve the learning efficiency and accuracy in spiking neurons, membrane potential-driven methods emerged recently. Typical examples of these methods include the Tempotron [31], PBSNLR [32], HTP [33] and EMPD [34]. Compared with their spike-driven counterparts, they take an entirely different approach where the relevant signal for synaptic change is the postsynaptic membrane potential rather than spike times. For instance, the Tempotron implements a gradient descent dynamics that minimizes an error defined as the difference between the maximum membrane potential and the firing threshold. However, this reliance on the maximum membrane potential as its objective function prevents the binary Tempotron learning rule from controlling the number of spikes beyond one [35]. PBSNLR [32] and HTP [33] perform a perceptron classification on discretely sampled time points of the membrane potential, with the aim to keep membrane potential below threshold at undesired spike times and to make sure a threshold crossing occurs at desired spike times [36]. As they are based on the perceptron learning rule, in theory, if the sampled time points of the membrane potential are not linearly separable, the desired output spike train cannot be learned successfully [32]. In addition, when the time step is small, the memory usage of the training samples as well as the training time increase greatly [32]. EMPD employs two different error functions at desired and undesired output time and uses gradient descent method to adjust the synaptic weights. However, EMPD [34] imposes additional restrictions on the spiking neuron model, and the calculation of monitoring time points (MPs) is time consuming. Therefore, more performance improvements are still needed for this type of learning methods.

Another important aspect often overlooked when designing learning strategies for spiking neural networks is the robustness to noise. Noise is common in spiking neural networks and can significantly affect the learning performance as well as the timing accuracy and reliability of neural responses [37]-[39]. In order to improve noise robustness of the trained neurons, most of the existing supervised learning methods use noisy samples during the training phase (i.e., noisy training) [23], [32]. However, the neurons trained under noisy conditions are found to show relatively robust responses only to the stimuli

used during the training phase, and their response to other stimuli not seen during the training is highly unreliable [23]. Therefore, improving the robustness of learning methods for spiking neurons remains an open problem.

In order to address the above mentioned limitations of existing supervised learning methods for spiking neurons, we propose in this paper a novel highly effective and noise robust membrane potential driven supervised learning method for spiking neurons with significant improvement in the learning efficiency. The proposed learning method, called MemPo-Learn (MEMbrane POTential driven supervised LEARNING), is able to generate desired spike trains with higher accuracy, higher efficiency and better robustness to input jitter as well as voltage noise. The efficiency of the MemPo-Learn is significantly improved through the introduction of an adaptive strategy, called Skip Scan Training Strategy (SSTS), which enables the MemPo-Learn method to accurately and efficiently learn the desired output spike train even when much smaller time steps are used. In addition, we analyse the noise robustness of the proposed MemPo-Learn method and introduce further improvements to make it significantly more robust to noise. The performance of the proposed learning method is thoroughly evaluated on synthetic data and is further demonstrated on real world classification tasks. Experimental results demonstrate that the proposed method is superior to other supervised methods in terms of the three key performance factors of supervised learning for spiking neurons, namely learning accuracy, learning efficiency, and robustness to noise.

The remainder of this paper is organised as follows: Section II introduces the neuron model and the learning rule of the proposed MemPo-Learn method. Section III and IV present a detailed description of the proposed strategies for improving the efficiency and noise robustness of MemPo-Learn. Section V presents a comprehensive experimental evaluation of the proposed MemPo-Learn method on synthetic spatio-temporal data including extensive experiments to explore the effect of different learning parameters on its learning performance. Further demonstration of the proposed learning method on real world applications are also presented in this section. Finally, Section VI discusses the results and draw conclusions.

II. THE MEMPO-LEARN LEARNING RULE

In this section, we begin by presenting the neuron model. Then, the main idea of MemPo-Learn learning rule is described.

A. Neuron model

There are many spiking neuron models that aim to capture the dynamics of biological neurons [12], [40], [41]. The spike-response model (SRM) offers a generalization of the integrate-and-fire model and can give a faithful description of biological neurons [12]. In addition, the SRM model is easily reducible to a numerical method that can be implemented on a computer; hence it is used in this paper.

In the SRM model, the membrane potential of a neuron i is represented by a variable u_i which remains at the resting potential, $u_{rest} = 0$, when there is no spike received from the

presynaptic neurons. When a spike produced at a pre-synaptic neuron j , a postsynaptic potential (PSP) is induced in neuron i . After the integration of the PSPs resulting from several incoming spikes, the post-synaptic neuron i fires a spike when its membrane potential u_i reaches a certain firing threshold ϑ . Let's suppose neuron i has fired its last spike at time \hat{t} . After firing the evolution of u_i is given by

$$u_i(t) = \eta(t - \hat{t}) + \sum_j \omega_{ji} \sum_f \varepsilon_{ji}(t - t_j^f) + u_{rest} \quad (1)$$

where t_j^f is the f th spike of presynaptic neuron j , and ω_{ji} is the synaptic weight from neuron j to neuron i . The PSP induced by the spike t_j^f is determined by the spike response function $\varepsilon_{ji}(t - t_j^f)$ defined as

$$\varepsilon_{ji}(t - t_j^f) = \begin{cases} \frac{t - t_j^f}{\tau} \exp(1 - \frac{t - t_j^f}{\tau}), & \text{if } t - t_j^f > 0 \\ 0, & \text{otherwise.} \end{cases} \quad (2)$$

where τ is a time decay constant that determines the spread shape of the spike response function. The refractoriness function $\eta(t - \hat{t})$ is defined as

$$\eta(t - \hat{t}) = \begin{cases} -\lambda \cdot \vartheta \exp(-\frac{t - \hat{t}}{\tau_R}), & \text{if } t - \hat{t} > 0 \\ 0, & \text{otherwise.} \end{cases} \quad (3)$$

τ_R is a time decay constant and λ is a constant that determines the amplitude of the refractoriness function. An illustration of the output produced by this neuron model in response to spatio-temporal spiking pattern is shown in in Fig. 1.

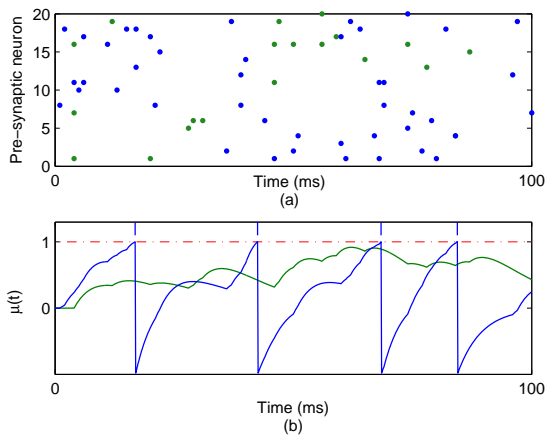


Fig. 1. Dynamics of the neuron model. (a) Examples of two input patterns (blue and green). Each input spike is represented by a dot. (b) Neuron response to the two input spiking patterns in (a). Blue trace: the neuron response to produce four spikes. Green trace: The neuron did not fire at all.

B. MemPo-Learn Learning Rule

The goal of supervised learning for spiking neurons is that the adjustable synaptic weights are modified to make an output neuron emit a desired spike train in response to a given input

spike pattern. Therefore, the running time of an output spiking neuron i can be divided into two sets: the times of desired output spikes denoted by t_d ($t_d = \{t_d(1), t_d(2), \dots, t_d(i), \dots\}$) and the remaining times, denoted by N_{td} . Based on these two different time classes, the proposed MemPo-Learn learning method employs two weight update processes: (1) Adjusting synaptic weights to make the membrane potential reach the firing threshold at desired output times t_d ; (2) Adjusting synaptic weights to maintain the membrane potential lower than the threshold at undesired output times N_{td} . These two weight update processes are introduced in the following sections.

1) *Weight Update Rule at Desired Output Spikes t_d* : For any time point in t_d , in order to fire a spike, the value of the neuron membrane potential is expected to cross the firing threshold from below. To achieve this, MemPo-Learn implements a gradient descent learning rule operating on the membrane potential at desired output times, with the aim to increase it towards the neuron firing threshold. When the membrane potential is below the firing threshold at desired output times, in order to make the membrane potential $u_i(t)$ reach the firing threshold ϑ , an error function is constructed as follows:

$$E_{t_d} = \begin{cases} \frac{1}{2}[u_i(t) - \vartheta]^2, & \text{if } u_i(t) < \vartheta, t \in t_d, \\ 0, & \text{otherwise.} \end{cases} \quad (4)$$

where ϑ represents the neuron firing threshold and $u_i(t)$ represents its postsynaptic membrane potential.

In gradient-based learning, changes in the synaptic weights are given by

$$\Delta\omega_{ji} = -\beta_1 \frac{\partial E_{t_d}}{\partial \omega_{ji}} \quad (5)$$

where β_1 is the learning rate which defines the size of the synaptic update at desired spiking times, and ω_{ji} is the synaptic weight from the presynaptic neuron j to the postsynaptic neuron i .

If the membrane potential $u_i(t)$ is below the firing threshold ϑ at desired output time, according to Eq. 5, synaptic weight ω_{ji} is increased by the following amount:

$$\Delta\omega_{ji} = -\beta_1 [u_i(t) - \vartheta] \sum_f \varepsilon_{ji}(t - t_j^f) \quad (6)$$

2) *Weight Update Rule at Undesired Output Spikes N_{td}* : For any time point in N_{td} , in order to avoid the occurrence of undesired output spikes, the membrane potential is required to remain below the neuron firing threshold. The proposed MemPo-Learn achieves this by again using a gradient descent learning rule. When the membrane potential is equal to or greater than the neuron firing threshold, to make the membrane potential $u_i(t)$ below the firing threshold ϑ , an error function at N_{td} is defined as Eq. (7)

$$E_{N_{td}} = \begin{cases} \frac{1}{2}[u_i(t) - (\vartheta - p)]^2, & \text{if } u_i(t) \geq \vartheta, t \in N_{td}, \\ 0, & \text{otherwise.} \end{cases} \quad (7)$$

where the parameter p determines the magnitude of modification on the synaptic weights at N_{td} . Then, the synaptic weights at N_{td} are updated according to the following equation:

$$\Delta\omega_{ji} = -\beta_2 \frac{\partial E_{N_{td}}}{\partial \omega_{ji}} \quad (8)$$

where β_2 is the learning rate, which defines the size of the synaptic update at undesired spiking times.

In order to drive the membrane potential below the threshold at N_{td} , the synaptic efficacy ω_{ji} is decreased by the following amount:

$$\Delta\omega_{ji} = -\beta_2[u_i(t) - (\vartheta - p)] \sum_f \varepsilon_{ji}(t - t_j^f) \quad (9)$$

C. Correlation-Based Metric.

To quantitatively evaluate the learning performance, a correlation-based, metric introduced in [42], is adopted to measure the similarity between the desired and actual output spike trains. The metric, defined in Eq. 10, is calculated after each learning epoch as follows:

$$C = \frac{\vec{v}_d \cdot \vec{v}_o}{|\vec{v}_d| |\vec{v}_o|}, \quad (10)$$

where \vec{v}_d and \vec{v}_o are vectors representing a convolution (in discrete time) of desired and actual output spike trains with a low-pass Gaussian filter. $\vec{v}_d \cdot \vec{v}_o$ is the inner product, and $|\vec{v}_d|$ and $|\vec{v}_o|$ are the Euclidean norms of \vec{v}_d and \vec{v}_o , respectively.

The Gaussian filter function with parameter σ is given by

$$f(t, \sigma) = \exp\left(\frac{-t^2}{2\sigma^2}\right) \quad (11)$$

where the parameter σ determines the width of the function. In this paper, σ is set to 2. The closer the value of C is to 1, the more similar the two spike trains with a value of $C = 1$ indicating identical spike trains. On the other hand, the closer the value of C is to 0, the less similar (i.e. weakly correlated) the two spike trains.

III. ENHANCING MEMPO-LEARN EFFICIENCY THROUGH THE SKIP SCAN TRAINING STRATEGY (SSTS)

In this section, we first analyse the effect of using a small time step on the learning complexity then we propose a strategy, called Skip Scan Training Strategy (STSS), which helps improve both the effectiveness and the efficiency of MemPo-Learn when small time steps are used to calculate the neuron dynamics.

A. Learning with a small time step

Fig. 2a shows that using a time step of 1 ms, the membrane potential has been kept below the threshold (i.e. $u < \vartheta$) at undesired spike times (namely time points 1, 2, 3, 5, 6, 7, ...) ms, and it has been pushed above the firing threshold (i.e. $u \geq \vartheta$) at desired output time (i.e. at time point 4 ms). As a result, a perfect learning of the desired output spiking time has been achieved. However, this learning may fail when a smaller time step (such as 0.01 ms) is used, **because** the threshold crossing of the membrane potential within $[t_1, t_2]$ and $[t_3, t_4]$

will occur at an undesired time (e.g. earlier than the desired time or **with** an additional undesired spike as illustrated in Fig. 2b). This time step related problem arises not because of the mathematical equations of spiking neuron model but the discrete-time simulation. In order to achieve a successful learning with a small time step, the update of synaptic weights should take the following constraints into account: (1) The membrane potential should remain below the firing threshold at all undesired output times; (2) The membrane potential at desired times t_d should equal to the firing threshold (as shown in Fig. 2c). However, like the existing learning methods, it is not easy for MemPo-Learn to meet these two constraints combined. The reasons are outlined below.

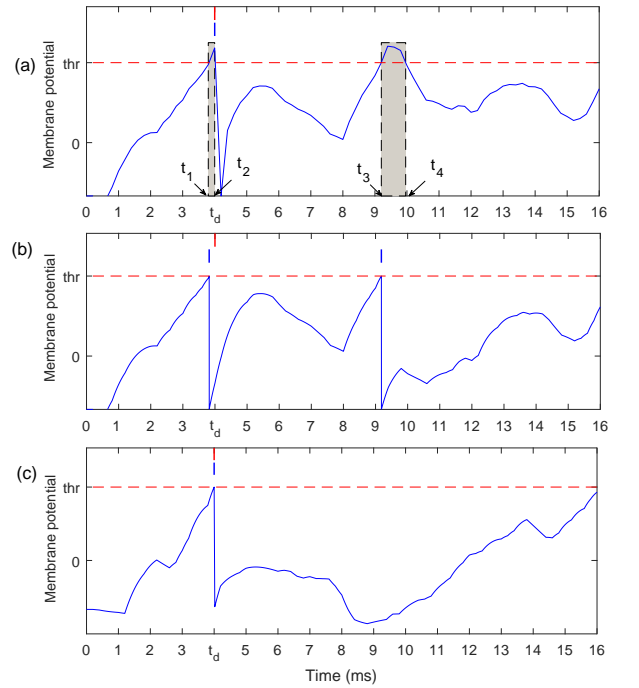


Fig. 2. Learning performance is related to time step. (a) Membrane potential trace after a successful learning with a time step of 1 ms. Desired output time t_d and actual output time are marked by red vertical bar and blue vertical bar, respectively. (b) When the time step is 0.01 ms, the threshold crossing of the membrane potential within $[t_1, t_2]$ and $[t_3, t_4]$ will produce undesired spikes. (c) Membrane potential trace after a successful learning with a time step of 0.01 ms.

1) *Over-Adjustment at N_{td}* : Fig. 3 shows the membrane potential trace of a neuron before learning, in which the membrane potential is above threshold when $t \in [53, 70]$ ms (as depicted by the grayed area). In order to push the membrane potential below the firing threshold with a smaller time step, as shown in Fig. 3(b), the synaptic weight will need to be adjusted continuously and be decreased great deal to be brought below the firing threshold. This over-adjustment at N_{td} may also drive the membrane potential much lower than the firing threshold at desired spiking times t_d , and also results in a much increased synaptic weights needed at desired spiking times t_d .

2) *Inadequate Learning for t_d* : The use of the error function proposed in Eq. 4 for synaptic update results in the membrane potential exceeding the firing threshold at desired

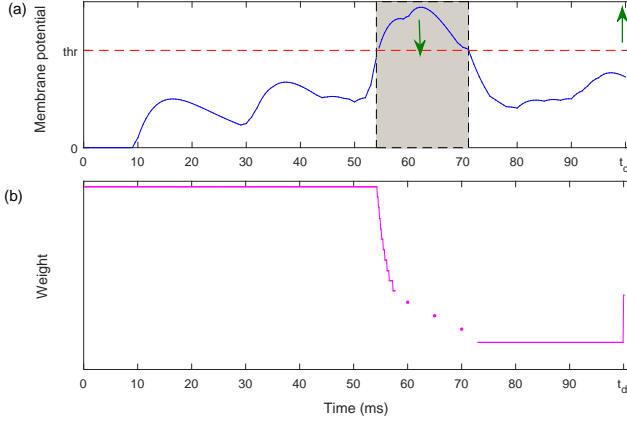


Fig. 3. Learning with a smaller time step is easy to fall into over-adjustment. (a) The membrane potential is above threshold at N_{td} (as depicted by the grayed area). (b) Weight changing during one learning epoch. To make the membrane potential below the threshold at N_{td} , the synaptic weight is decreased too much after one learning epoch

spiking times t_d (i.e. $u(t_d) \geq \vartheta$). However, when a smaller time step is used, the membrane potential at t_d is required to equal to the firing threshold. Therefore, we use a modified form of Eq. 4 as follows

$$E_{t_d} = \frac{1}{2}[u_i(t) - \vartheta]^2 \quad \text{if } t \in t_d. \quad (12)$$

It is easy to find that making membrane potential exactly equal to the firing threshold at desired spiking times t_d is difficult, and more learning opportunities should be given to t_d . However, all the existing learning methods give only one learning chance to t_d during one learning epoch. Inadequate learning for t_d is one of the reasons that make a small time step learning time-consuming.

B. Skip Scan Training Strategy (SSTS)

The SSTS strategy is proposed to address over-adjustment at undesired spike times N_{td} and inadequate learning at desired output times t_d . The reason of over-adjustment is that, with a small time step, the synaptic weights would be decreased continuously. To avoid this, SSTS divides one learning epoch into many sub-epochs. In each sub-epoch, MemPo-Learn skips a period of time denoted by s_{len} to train the synaptic weights. On the other hand, in order to guarantee enough learning opportunities at t_d , the MemPo-Learn is applied to update the synaptic weight at t_d in each sub-epoch. The meanings of the symbols used in SSTS and the detailed pseudocode of the SSTS are shown below.

TABLE I
MAIN SYMBOLS USED IN SSTS

Symbols	Means
s_t	The starting time point of desired output spike train
t_s	The simulation time step
t_f^n	The first training time point of n th sub-epoch
$Sub(n)$	The set of all the training time points in n th sub-epoch
s_{len}	A fixed time length of skip.
T	The length of the desired output spike train;
$t_d(i)$	The i th spike of the desired output time.

The MemPo-Learn rule combined with SSTS

```

1) Divide one learning epoch into many sub-epochs according to SSTS
For  $n = 1 : 1 : s_{len}/t_s$ 
  a) Choosing the first training time point of  $n$ th sub-epoch:
      $t_f^n = s_t + (n - 1)t_s$ ;
  b) Continue to add  $s_{len}$  to get other training time points until we reach
     the end of the spike train  $T$ :
      $Sub(n) = [t_f^n, t_f^n + s_{len}, t_f^n + 2 \times s_{len}, t_f^n + 3 \times s_{len}, \dots]$ ;
  c) Add all the desired output times into the training time points of each
     sub-epoch:
      $Sub(n) = [t_f^n, t_f^n + s_{len}, t_d(1), t_f^n + 2 \times s_{len}, t_f^n + 3 \times s_{len}, t_d(2), \dots]$ ;
EndFor
2) Update synaptic weights according to the MemPo-Learn rule
For  $n = 1 : 1 : s_{len}/t_s$ 
  For  $i = 1 : 1 : \text{length}(Sub(n))$ 
    if  $Sub(n, i) \in t_d$ 
      Update synaptic weight according to Eq. (12) and Eq. (6);
    Endif
    if  $Sub(n, i) \notin t_d$ 
      Update synaptic weight according to Eq. (7) and Eq. (8);
    Endif
  Endfor
Endfor

```

To illustrate the proposed SSTS strategy more clearly, an example of SSTS is shown in Fig. 4. The parameters are set as follows: $s_t = 0.01$ ms, $t_s = 0.01$ ms, $s_{len} = 2$ ms, $T = 10$ ms. The steps for generating training time points in each sub-epoch are shown in Table. II. In the n th sub-epoch, $s_t + (n - 1)t_s$ is chosen as the first training time point, and the training time points in the n th sub-epoch can be obtained in the same way. It is easy to find when $n = s_{len}/t_s = 2/0.01 = 200$, SSTS reaches the last sub-epoch, and one learning epoch is completed.

TABLE II
MAIN STEPS TO GENERATE TRAINING TIME POINTS IN EACH SUB-EPOCH

$Sub(1)$	a) The first training time point: $t_f^1 = s_t + (n - 1)t_s = 0.01$ ms; b) Continue to add s_{len} to get other training time points: $Sub(1) = \{0.01, 2.01, 4.01, 6.01, 8.01\}$ ms; c) Insert all of the desired output times $t_d(1), t_d(2)$: $Sub(1) = \{0.01, 2.01, 4.01, t_d(1), 6.01, 8.01, t_d(2)\}$ ms.
$Sub(2)$	a) The first training time point: $t_f^2 = s_t + (n - 1)t_s = 0.02$ ms; b) Continue to add s_{len} to get other training time points: $Sub(2) = \{0.02, 2.02, 4.02, 6.02, 8.02\}$ ms; c) Insert all of the desired output times $t_d(1), t_d(2)$: $Sub(2) = \{0.02, 2.02, 4.02, t_d(1), 6.02, 8.02, t_d(2)\}$ ms.
...	...
$Sub(200)$	a) The first training time point: $t_f^{200} = s_t + (1 - 1)t_s = 2$ ms; b) Continue to add s_{len} to get other training time points: $Sub(200) = \{2, 4, 6, 8, 10\}$ ms; c) Insert all of the desired output times $t_d(1), t_d(2)$: $Sub(200) = \{2, 4, t_d(1), 6, 8, t_d(2), 10\}$ ms.

Fig. 4b shows the weight update process using SSTS, and Fig. 4c shows the weight update process without using SSTS.

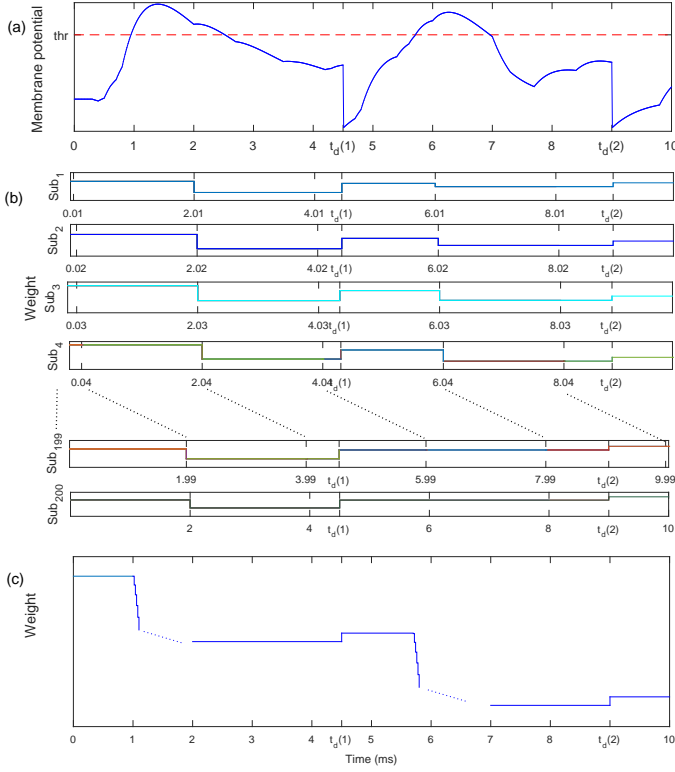


Fig. 4. An illustrative example of SSTS. (a) The membrane potential trace before learning. (b) The weight updating process using SSTS. (c) The weight update process without using SSTS. In this example, $s_t = 0.01$ ms, $t_s = 0.01$ ms, $s_{len} = 2$ ms.

In Fig. 4b, SSTS divides one learning epoch into many sub-epochs. In each sub-epoch, all desired output times are added into the training time points. In this way, inadequate learning for t_d is resolved. On the other hand, SSTS divides the continuous N_{td} period into many sub-epochs. In each sub-epoch, persistent decrease of synaptic weights is avoided, which resolves the problem of over-adjustment.

IV. IMPROVING THE ROBUSTNESS OF MEMPO-LEARN

In this section, we first analyse the robustness of MemPo-learn to noise, then we introduce a strategy that makes MemPo-Learn more robust to noise.

Noise is common in biologically plausible neural networks and can significantly affect the timing accuracy and reliability of the neural responses [37]-[39]. The noise disturbs the neuron response mainly by: (1) causing spurious spikes to appear or (2) by causing desired output spikes to vanish. It is easy to find that if the membrane potential is close to the firing threshold at N_{td} , the probability of triggering a wrong spike will increase. Therefore, in order to prevent the generation of additional undesired spikes, the membrane potential at N_{td} should be kept much lower than the firing threshold. **On the other hand**, to make sure that the neuron will fire nearby t_d , the membrane potential around t_d should be strong enough [23].

Based on the above analysis, as shown in Fig. 5, we divide the undesired output time N_{td} into two classes NT_f (far away

from a desired spike) and NT_n (near a desired spike):

$$NT_f = \{t | t_d(i) < t < t_d(i+1) - \delta\} \quad (13)$$

$$NT_n = \{t | t_d(i+1) - \delta \leq t < t_d(i+1)\} \quad (14)$$

where $t_d(i)$ and $t_d(i+1)$ denote the moment of the i th and $(i+1)$ th spike in the desired spike train. The parameter δ determines the length of NT_n and NT_f .

(1) When $t \in NT_f$, to avoid undesired firing, the membrane potential is expected to keep a big distance from the firing threshold. Therefore, the error function of MemPo-Learn at NT_f is modified as

$$E = \frac{1}{2}[u_i(t) - (\vartheta - p)]^2, \quad \text{if } u_i(t) \geq \vartheta - p, t \in NT_f \quad (15)$$

According to Eq. 15, if $u_i(t) \geq \vartheta - p$, the synaptic weights would be reduced to keep the membrane potential lower than the firing threshold **by** at least p .

(2) When $t \in NT_n$, the error function is defined as

$$E = \frac{1}{2}[u_i(t) - (\vartheta - p)]^2, \quad \text{if } u_i(t) \geq \vartheta, t \in NT_n. \quad (16)$$

Eq. 16 is different from Eq. 15, because the period of NT_n is close to the desired output time. **If** the membrane potential is kept much lower than the threshold it will make the spiking neuron hard to output a spike at t_d .

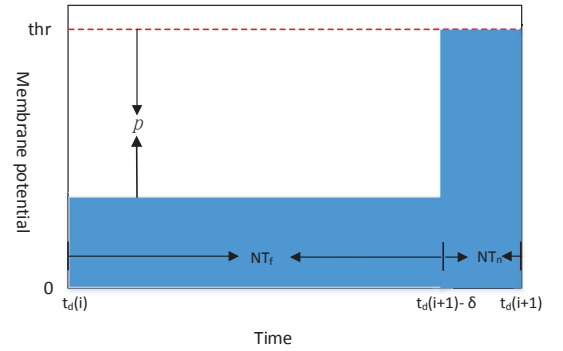


Fig. 5. Illustration of the robust MemPo-Learn. The undesired output time is divided into two classes: NT_n and NT_f . After a successful learning, the trace of the neuronal membrane potential only appears in the shaded part, which is far away from the firing threshold at NT_f and strong enough at NT_n .

The error function of the robust MemPo-Learn at t_d is similar to that of MemPo-Learn, i.e. it is also defined by Eq. 4, which ensures a threshold crossing at desired output times. After a successful learning with the robust MemPo-Learn, as shown in Fig. 5, the trace of the neuronal membrane potential only appears in the shaded part.

V. SIMULATION RESULTS

We conducted extensive experiments to thoroughly evaluate the performance of the proposed learning method and test its tolerance to parameter variation. We further demonstrate the proposed learning method on real world classification tasks.

A. Learning performance of MemPo-Learn

In this section, we investigate the effect of different parameters on the learning performance, including the length of spike trains, the number of the synaptic inputs and the firing rate of spike trains. We compare our method against competitive learning rules for spiking neurons, namely ReSuMe and PBSNLR which are typical learning methods of spike-driven methods and membrane potential-driven methods, respectively. In these simulations, the time step is set to 1 ms.

1) *Effect of the Spike Trains Length:* In these simulations, a neuron with 400 synaptic inputs is trained to reproduce a desired sequence of spikes. Every input spike train and the desired output spike train are generated according to a homogeneous Poisson process with firing rates of 10 Hz and 100 Hz, respectively. Each experiment is repeated for 20 trials for different input and desired output pairs. The initial synaptic weights are randomly drawn from the interval $[0, 0.05]$ using a uniform distribution. In Fig. 6, the length of the desired output spike trains varies from 400 ms to 2800 ms with an interval of 400 ms. The average maximum C value scored during training, the average number of epochs and the average computing time required to reach the maximum C are calculated and reported for benchmarking.

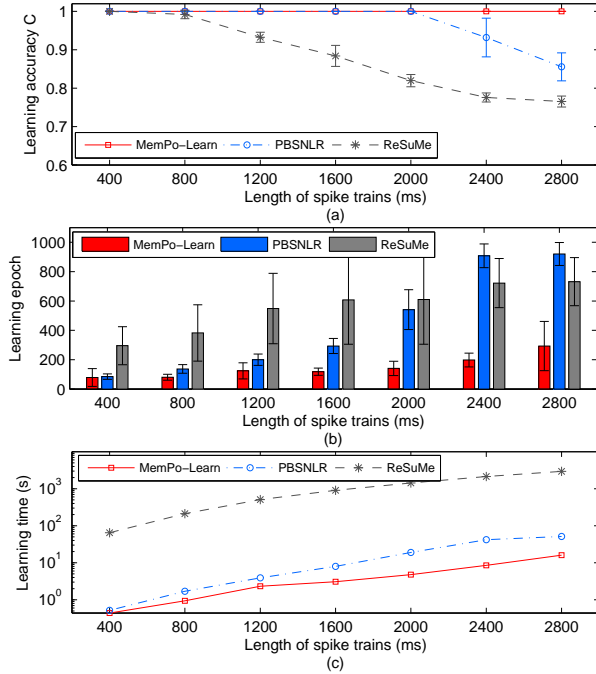


Fig. 6. The comparison of learning performance when the length of desired spike trains increases gradually. Time step=1 ms.

Fig. 6a illustrates the change in learning accuracies of MemPo-Learn, PBSNLR and ReSuMe. The learning accuracies of all the methods are very high (with C reaching 1) when the length of spike trains varies from 400 ms to 800 ms. While the learning accuracy for ReSuMe and PBSNLR starts declining when the length of spike train exceeds 1200 ms and 2000 ms, respectively, the learning accuracy of the

proposed MemPo-learn is maintained at $C = 1$ until the length of spike train exceeds 2800 ms. In addition, Fig. 6b shows that MemPo-Learn requires much fewer epochs than ReSuMe and PBSNLR in order to reach the maximum accuracy. For instance, for a spike train length of 2000 ms, ReSuMe and PBSNLR require about 600 learning epochs to reach the maximum value of C , while MemPo-Learn requires only about 200 learning epochs (i.e. a third of the number of epochs required by its competitors). Moreover, as shown in Fig. 6c, the learning time of MemPo-Learn and PBSNLR are much better than that of ReSuMe. In addition, the required learning time of MemPo-Learn is comparable with that of PBSNLR for short spike trains (up to 1200 ms) but it is clearly much lower for spike trains of duration greater or equal than 1600 ms. For example, PBSNLR learning takes almost four times longer than MemPo-Learn when the length of the spike train is 2400 ms, which is a significant improvement in learning efficiency.

2) *Effect of the Number of the Synaptic Inputs:* In this part, we investigate the effect of the number of synaptic inputs. The length of the input and the desired output spike train is set to 800 ms. Every input spike train and the desired output spike train are generated according to a homogeneous Poisson process with firing rates of 10 Hz and 100 Hz, respectively. The number of synaptic inputs varies from 50 to 500. The experimental results are shown in Fig. 7.

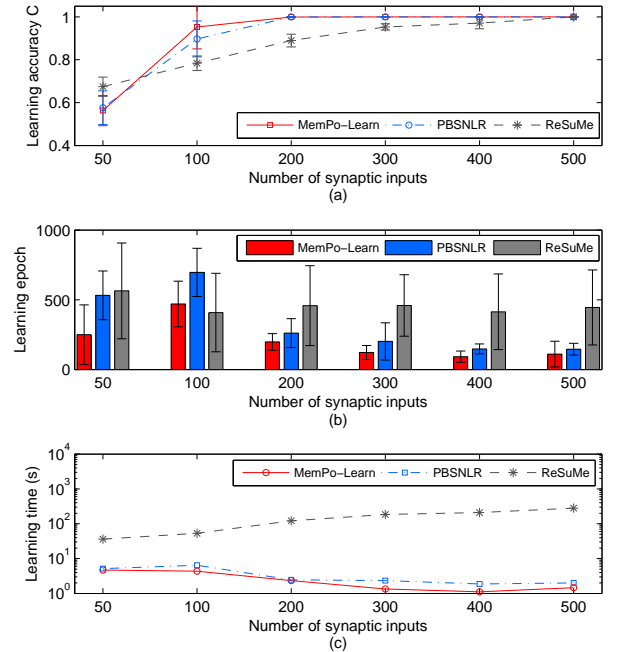


Fig. 7. The comparison of learning performance when the number of the synaptic input increases gradually. Time step=1 ms.

Fig. 7a shows that a small number of synaptic inputs results in a low learning accuracy for the three learning methods MemPo-Learn, ReSuMe and PBSNLR. However their learning accuracy increases with the increase of the number of synaptic inputs. MemPo-Learn can quickly reach a very high value of C (close to 1) using a relatively small number of synaptic inputs.

For example, when the number of synaptic inputs is 100, the learning accuracy of MemPo-Learn is almost 1, while the learning accuracies of ReSuMe and PBSNLR are much lower at 0.85 and 0.75, respectively. In terms of learning efficiency, Fig. 7b shows a downtrend in the required number of learning epochs for different methods. However, the number of required epochs for the proposed MemPo-Learn remains much lower than that of PBSNLR and ReSuMe irrespective of the number of inputs used. Fig. 7c clearly illustrates the superiority of MemPo-Learn in terms of the required learning time. Again, the learning efficiency of MemPo-Learn is better than that of PBSNLR and ReSuMe irrespective of the number of inputs. For example, when the number of synaptic input is 100, the learning time of ReSuMe, PBSNLR and MemPo-Learn are 53.1 s, 6.4 s and 4.3 s, respectively.

3) *Effect of the Firing Rate of the Spike Trains*: The following experiments aim to evaluate the effect of the firing rate of the spike trains. The firing rates of the input spike trains (F_{in}) vary from 2 Hz to 18 Hz with an interval of 4 Hz. The firing rates of the desired output spike trains (F_{out}) vary from 20 Hz to 160 Hz with an interval of 20 Hz. The number of the synaptic inputs is 400, and the length of the spike trains is 800 ms. The learning is continued for 1000 learning epochs, and the maximum obtained learning accuracy is reported in Fig. 8.

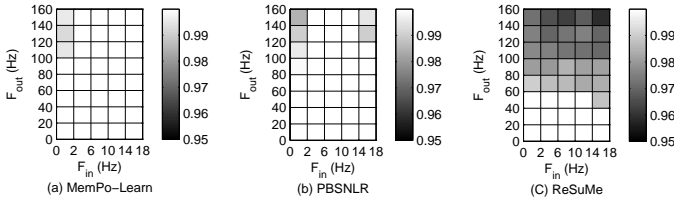


Fig. 8. The comparison of learning performance when the firing rates of the input and desired output spike trains increase gradually. Time step=1 ms.

From Fig. 8, MemPo-Learn, PBSNLR and ReSuMe reach the highest learning accuracy for the lowest value of F_{out} , and there is a trend that the learning accuracies of all methods decrease with the increase of F_{out} . On the other hand, the area in which MemPo-Learn achieves high performance is larger than that of PBSNLR and ReSuMe. For example, when $F_{in} = 18$ Hz, the performance of MemPo-Learn is 1 for all values of F_{out} in [20, 160] Hz. However, in the case of $F_{in} = 18$ Hz, the learning accuracy of PBSNLR is 1 only when F_{out} in [20, 120] Hz, and the learning accuracy of ReSuMe is 1 only when F_{out} in [20, 40] Hz.

B. Learning Performance of MemPo-Learn combined with SSTS

In this section, we investigate the learning performance of MemPo-Learn combined with SSTS with a time step of 0.01 ms.

1) *Effect of the Time Step*: In the following experiments, a neuron with 400 input synapses is trained to emit a desired sequence of spikes with a length of 400 ms. Every input spike train and desired output spike train are generated randomly according to the homogeneous Poisson process with firing

rates of 10 Hz and 100 Hz, respectively. Each experiment is repeated for 20 trials for different input and desired output pairs, and average learning accuracy C in each learning epoch is reported. The experimental results are shown in Fig. 9.

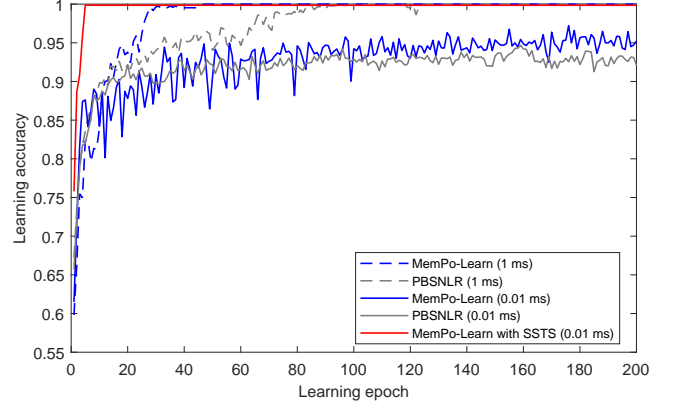


Fig. 9. The comparison of learning performance with different time step

From Fig. 9, when time step is 1 ms, both MemPo-Learn and PBSNLR reach a value of $C = 1$ at epochs of 47 and 124, respectively, then the learning parameters become stable. In this case, MemPo-Learn reaches $C = 1$ after 47 epochs which amounts to $47 \times 0.006 = 0.282$ s, and PBSNLR reach $C = 1$ after 124 epochs which amounts to $124 \times 0.0058 = 0.719$ s. The learning performance of MemPo-Learn and PBSNLR drops significantly with a time step of 0.01 ms. For instance, the C value for MemPo-Learn (0.01 ms) at epoch 47 is 5% lower than that obtained using a time step of 1 ms, and the C value for PBSNLR (0.01 ms) at epoch 124 is 6% lower than that obtained using a time step of 1 ms. Moreover, both MemPo-Learn and PBSNLR are unable to reach $C = 1$ even if it is allowed to run for as long as 1000 learning epochs, which take a total of $1000 \times 0.67 = 670$ s for MemPo-Learn, and $1000 \times 0.66 = 660$ s for PBSNLR. Therefore, with a small time step, MemPo-Learn and PBSNLR's learning accuracy drops and the required number of learning epochs as well as the learning time increase. These observations confirm our theoretical prediction that the time step greatly affects the learning performance. On the other hand, the learning efficiency of MemPo-Learn combined with SSTS is significantly improved. For example, MemPo-Learn combined with SSTS can reach a learning high accuracy (C close to 1) after only 5 epochs which amounts to learning time of $5 \times 0.93 = 4.65$ s.

2) *Effect of the Spike Trains Length*: In these simulations, the number of synaptic inputs is 400. Every input spike train and the desired output spike train are generated according to a homogeneous Poisson process with rates of 10 Hz and 100 Hz, respectively. The length of the desired output spike trains varies from 100 ms to 800 ms with an interval of 100 ms, and the time step is set to 0.01 ms.

As shown in Fig. 10, MemPo-Learn combined with SSTS achieves better learning performance than MemPo-Learn, PBSNLR and ReSuMe. The learning accuracy of MemPo-Learn combined SSTS is higher than that of the other methods when the spike train length varies from 100 ms to 800 ms. For

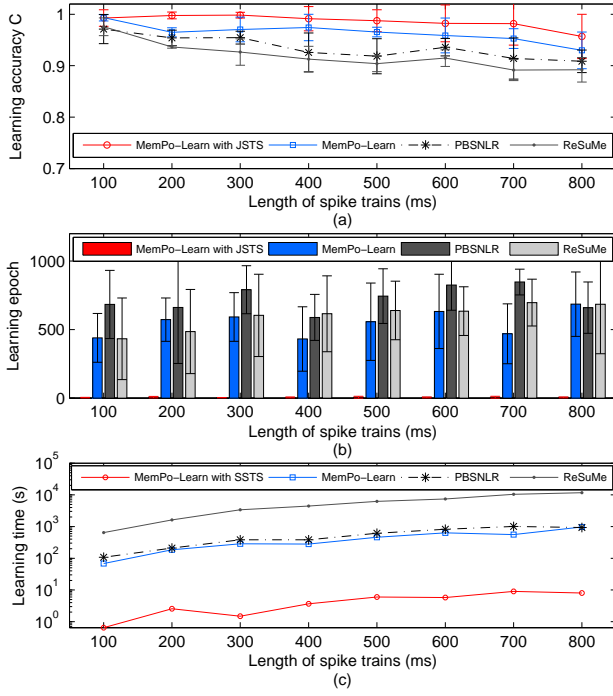


Fig. 10. The comparison of learning performance when the length of desired spike trains increases gradually. Time step=0.01 ms.

example, when the length of the desired spike train is 700 ms, the average learning accuracy of MemPo-Learn combined with SSTS is about 0.98, while the learning accuracies of MemPo-Learn, PBSNLR and ReSuMe are about 0.95, 0.93 and 0.91, respectively. Moreover, the required learning epochs and learning time for MemPo-Learn combined with SSTS are much lower. For example, when the length of spike trains is set to 700 ms, MemPo-Learn takes almost 60 times longer than MemPo-Learn combined with SSTS to complete learning, PBSNLR takes almost 110 times longer. Thus, the learning efficiency of MemPo-Learn combined with SSTS is clearly improved in comparison with MemPo-Learn without SSTS and PBSNLR.

3) *Effect of the Number of the Synaptic Inputs:* In the following experiments, the performance of MemPo-Learn combined with SSTS is evaluated for various values of the number of the synaptic inputs 500, 400, 300, 200, 100, 50. In these simulations, the length of spike train is 400 ms, and the time step is 0.01 ms. Every input spike train and the desired output spike train are generated according to a homogeneous Poisson process with rates of 10 Hz and 100 Hz, respectively.

From Fig. 11, when the number of synaptic inputs varies from 50 to 100, we can see that the learning accuracy curves of different methods are comparable. However, when the number of synaptic input exceeds 200, the learning accuracy of MemPo-Learn combined with SSTS is overall higher than that of other methods. When the number of synaptic inputs is 500, the learning accuracy of MemPo-Learn combined with SSTS is very high (measure C is almost equal to 1), while the highest learning accuracy of other three methods is only

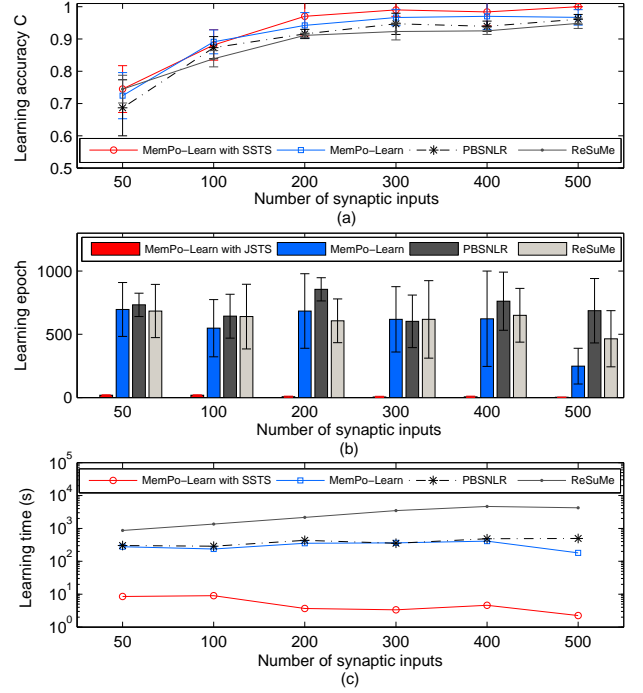


Fig. 11. The comparison of learning performance when the number of the synaptic input increases gradually. Time step=0.01 ms.

0.96. As for learning efficiency, the proposed MemPo-Learn combined with SSTS remarkably outperforms both MemPo-Learn, PBSNLR and ReSuMe in terms of both required number of epochs as well as required learning time. This is clearly reflected in a dramatic reduction in both the required number of epochs, which is illustrated by the red bars in Fig. 11b, and the required learning time which is illustrated by the red curve in Fig. 11c. For example, when the number of synaptic inputs is 500, the required number of learning epochs for MemPo-Learn, PBSNLR and ReSuMe are 248, 686 and 468, respectively. However, MemPo-Learn combined with SSTS requires only about 3 learning epochs which clearly is an impressive improvement.

4) *Effect of the Firing Rate of the Spike Trains:* In the following experiments, we aim to evaluate the effect of the firing rate of the spike trains. The firing rates of the input spike trains (F_{in}) vary from 6 Hz to 18 Hz with an interval of 4 Hz. The firing rates of the desired output spike trains (F_{out}) vary from 20 Hz to 160 Hz with an interval of 20 Hz. The number of the synaptic input is 400, and the length of the spike trains is 400 ms. The learning is continued for 1000 learning epochs, and the maximum obtained learning accuracy is reported in Fig. 12.

From Fig. 12, all of the learning methods reach their highest learning accuracy when $F_{in} = 6$ Hz and $F_{out} = 20$ Hz. When $F_{in} = 18$ Hz and $F_{out} = 160$ Hz, all of these three methods reach their lowest values of performance. On the other hand, the area in which MemPo-Learn combined with SSTS achieves high learning accuracy is larger than that of other methods.

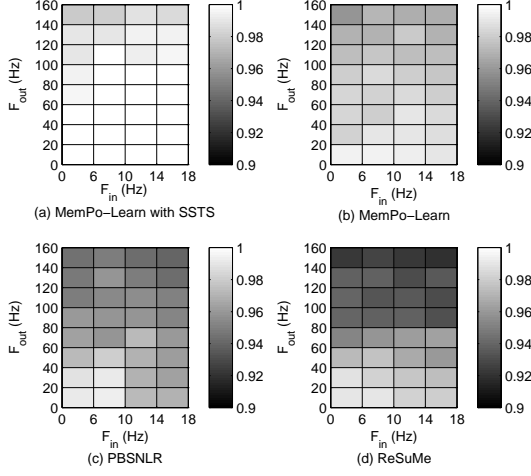


Fig. 12. The comparison of learning performance when the firing rates of the input and desired output spike trains increase gradually. Time step=0.01 ms.

C. Robustness to Noise

In this part, we investigate the noise robustness of the neuron trained by different learning methods. A neuron with 400 synaptic inputs is trained to output the desired spike train with a length of 800 ms. Every input spike train and the desired output spike train are Poisson spike trains with rates 10 Hz and 100 Hz, respectively. After training, the reliability of the target recall is tested against two noise cases: 1) background noise on the membrane potential, and 2) input jittering noise.

1) *Robustness to Membrane Potential Noise:* In this case, background membrane potential noise is considered as the noise source. After training, the trained neuron is subjected to simulated background Gaussian white noise. The mean value of the added noise is 0, and its variance σ_b is systematically increased within the range of [0.03, 0.33] mV. For each value σ_b , 20 experiments are carried out. A correlation measure C [42] of a distance between the desired and actual output spike trains is calculated. The experimental results are shown in Fig. 13.

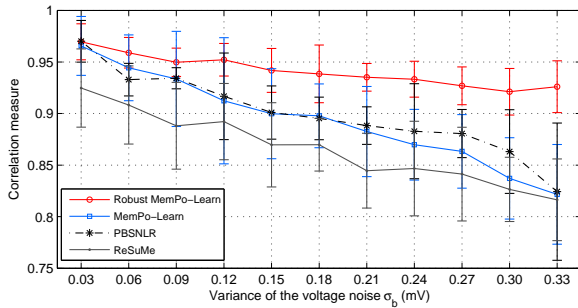


Fig. 13. Anti-noise capability of different learning algorithms against background voltage noise.

Fig. 13 shows that the correlation C of all the three methods is high when the intensity of noise is small. However, it decreases when the noise intensity is gradually increased. The correlation C curves of MemPo-Learn, PBSNLR and ReSuMe decline relatively early and quickly. However, the correlation

C of the neuron trained by R-MemPo-Learn always maintains high values with the increase of σ_b , and is significantly higher than other methods. These results confirm that the neuron trained by R-MemPo-Learn is significantly less sensitive to noise.

2) *Robustness to Input Spike Time Jitter:* In this case, input jittering noise is considered as the noise source. After learning, we jitter the input spike times. The jitter intervals are randomly drawn from a Gaussian distribution with mean 0 and variance $\sigma_j \in [0.3, 3.3]$ ms. In addition, some spikes are randomly removed (with a probability of 0.05) or added (at the times generated by a 1Hz homogeneous Poisson process). The resulting plots of C are presented in Fig. 14.

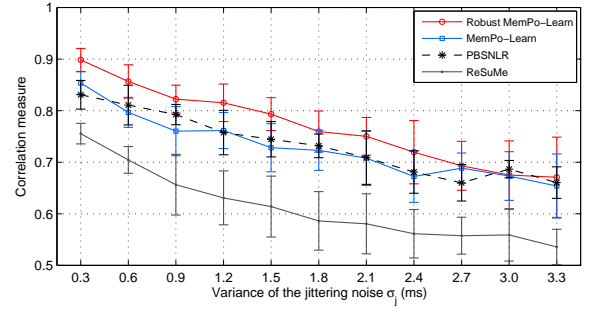


Fig. 14. Anti-noise capability of different learning algorithms against jittering noise.

As shown in Fig. 14, as the intensity of noise increases, the noise greatly reduces the degree of correlation between the desired and the actual output spike trains. The measure C scored by MemPo-Learn, PBSNLR and ReSuMe drops more sharply than that of the robust MemPo-Learn. That is, neuron trained by the robust MemPo-Learn is clearly more robust to noise than the neuron trained by other methods.

D. Effect of Learning Parameters p and s_{len}

Two major learning parameters involved in our method are p and s_{len} . In this section, we aim to investigate the effect of these parameters on the learning performance.

1) *Effect of Parameter p :* The role of p is to make the membrane potential below the firing threshold at undesired firing times N_{td} . It determines the magnitude of modification on the synaptic weights at N_{td} . To look into the effect of p , we conduct several experiments with a time step of 1 ms. A neuron with 200 synaptic inputs is trained to emit a desired sequence of spikes with a length of 500 ms. Every input spike train and desired output spike train are generated randomly according to a homogeneous Poisson process with rate $r = 10$ Hz and 100 Hz, respectively. Here we choose $p=0.01, 0.05, 0.1, 1, 3, 6$ and 9 mv. If the number of learning epochs exceeds 500, we regard this training as a failure. The accuracy value C and the number of epochs needed to reach C are shown in Table III.

Table III reveals that C equals 1, though the values of p range from 0.01 mv to 6 mv, and it means that MemPo-Learn has the advantage of parameter insensitivity. A larger p can result in a faster learning speed, but when p is increased

TABLE III
THE IMPACT OF p ON THE LEARNING PERFORMANCE.

p	0.01	0.05	0.1	1	3	6	9
C	1	1	1	1	1	1	Failure
Epochs	87	79	65	92	119	189	-

above a critical value (e.g., 0.1 mv in our experiments), the learning will slow down or even fail. A smaller p means a smaller adjustment for synaptic weights, which results in more learning epochs. Weight updating inevitably changes not only the membrane potential at current time but also the membrane potential at other times, so it will affect the precious learning results. A larger p has a bigger interference on the previous learning results, and it results in more learning epochs. Moreover, if the value of p is too large, the learning process will fall into over-adjustment or even fail.

2) *Effect of Parameter s_{len}* : We have proposed the SSTS strategy to resolve the problems of over-adjustment and inadequate learning chances at t_d . The most important parameter in SSTS is s_{len} . To investigate the effect of s_{len} , we conduct several experiments with a setup similar to Table III but with a time step of 0.01 ms and the neuron is trained by MemPo-Learn combined with SSTS. The parameter s_{len} is varied between 1 and 7 with a unit step (i.e. $s_{len} = 1, 2, 3, 4, 5, 6, 7$ ms). If the number of learning epochs exceeds 10, we regard this training as a failure. The value of accuracy C and the number of epochs needed to reach it are shown in Table IV.

TABLE IV
THE IMPACT OF s_{len} ON THE LEARNING PERFORMANCE.

s_{len}	1 ms	2 ms	3 ms	4 ms	5 ms	6 ms	7 ms
C	1	1	1	1	1	1	1
Epochs	5	3	3	2	1	1	1

As shown in Table IV, s_{len} has little effect on accuracy since the values of C are all equal to 1. A large s_{len} results in a smaller number of learning epochs, but when s_{len} is increased above a critical value (e.g., 5 ms in our experiment), the number of learning epochs keeps the same. For SSTS, the number of sub-epochs $n = s_{len}/t_s$, a larger s_{len} means more sub-epochs. According to SSTS, the times of desired output spikes are added into each sub-epoch. So a larger s_{len} will give more learning chances to t_d . When s_{len} is large enough, t_d has adequate learning chances to make the membrane potential equal to the threshold. In this case, if we continue to increase the value of s_{len} , it may not do much to raise the learning speed.

E. Classification

Spiking neural networks have been applied to various classification tasks [45]-[56]. In most case, the spiking neuron based classifiers make decisions using single spike only [25], [31], [46]-[48] or by using analog or binary signal representation [23], [51]. Only a few of the spiking neuron based classifiers considered the ability to represent the classified categories by

the corresponding sequences of precisely timed firing. Here, we illustrate this ability of our method in a classification task proposed by Qiang Yu and Huajin Tang [54], [55], where a spiking neuron based computational model (as shown in Fig. 15) is proposed for spike sequences classification. In this experiment, we adopt this computational model to evaluate the capability of the proposed learning method in practical applications, including optical character recognition and sound event classification.

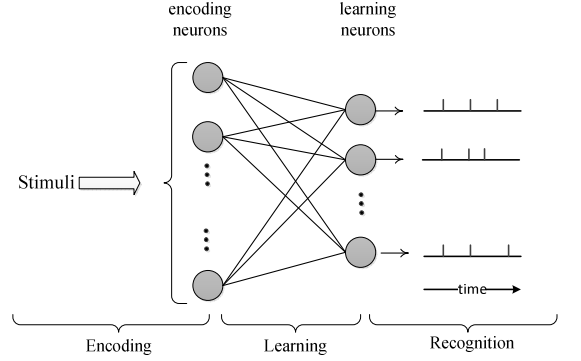


Fig. 15. General structure and information process of the SNN. It contains three functional parts: encoding, learning, and recognition. The encoding part is used to convert the input patterns into different spike trains. The learning part tunes the synaptic weights to ensure that the output part can respond to certain patterns correctly. The readout part extracts information about the stimulus from a given neural response.

1) *Optical Character Recognition*: An Optical Character Recognition (OCR) task is considered in this experiment where images of digits 0-9 are used. Each image has a size of 20×20 black/white (B/W) pixels. Sample images are shown in Fig. 16a. In the encoding part, a phase encoding method is used to convert the images into spatiotemporal spike patterns [54], [55]. The mechanism of the phase encoding is shown in Fig. 16b. Each encoding unit consists of a positive neuron (Pos), a negative neuron (Neg) and an output neuron. Each encoding neuron is assigned to a pixel and a subthreshold membrane potential oscillation (SMO). (More details about phase coding, please see references [54], [55]).

The learning part of the spiking neural network is composed of one layer of 10 spiking neurons, with each learning neuron corresponding to one category. Each learning neuron is trained to fire a desired sequence of spikes ([40, 80, 120, 160] ms) when a corresponding pattern is present, and not to spike when other patterns are presented.

In the recognition part, the relative confidence criterion is used for decision making, where the input pattern will be decided by one of the neurons that generates the most similar spike train to the target spike train.

After phase coding, different images can be converted into corresponding spatiotemporal spike patterns. Fig. 17a demonstrates an encoding result of a given image sample, in which the output spikes are sparsely distributed over the encoding time window. To further illustrate the learning process of the MemPo-Learn rule, Fig. 17b shows the learning performance of digit "8". The learning neuron corresponding to digit "8" can successfully produce the desired spike train after about 25 learning epochs.

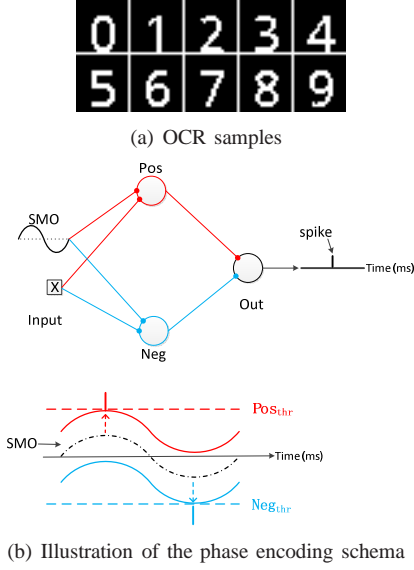
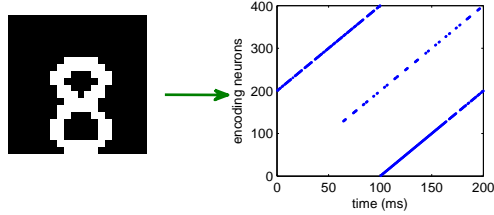
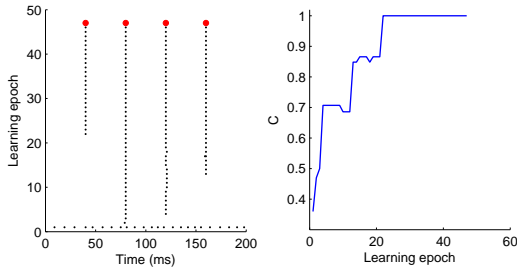


Fig. 16. (a) OCR samples. (b) Illustration of the phase encoding schema. Each encoding unit is assigned with a subthreshold membrane potential oscillation (SMO) and an input x . The encoding schema is adapted from [54], [55].)



(a) Phase encoding results of a given image sample. Each dot denotes a spike.



(b) Output spike signals of the learning neuron corresponding to digit “8”.

Fig. 17. Learning performance of the proposed method on the OCR recognition task.

To study the noise robustness of the proposed method on classification, after learning, the reliability of the target recall is tested against two noise cases: 1) background noise on the membrane potential; 2) input jittering noise. Fig. 18 and Fig. 19 show the classification accuracies of different learning algorithms against jittering noise and background voltage noise, respectively.

As can be seen from Fig. 18, the performance of all four methods decreases with increasing noise level. While both PBSNLR and MemPo-Learn without the noise robustness strategy show comparable response, the robust version of MemPo-Learn remarkably **outperforms** both MemPo-Learn

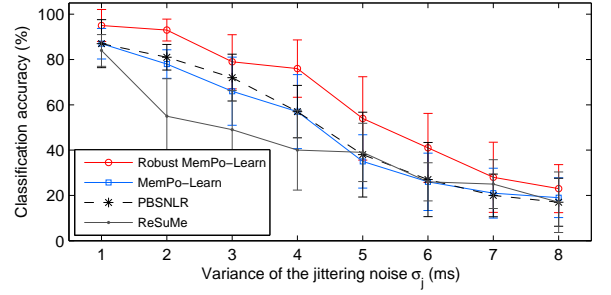


Fig. 18. Robustness of different methods against the jittering noise

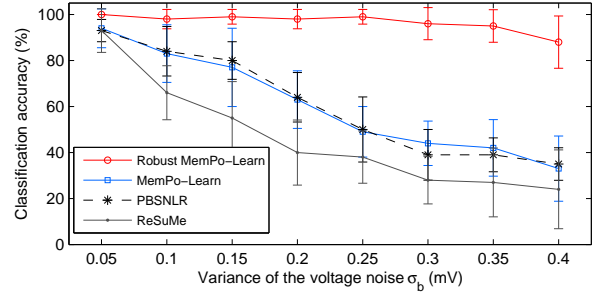


Fig. 19. Robustness of different methods against the background voltage noise

without the robustness strategy and PBSNLR. In addition, the robust of ReSuMe is relatively lower than that of other three methods.

From Fig. 19, we can see that when the intensity of noise is small, the classification accuracy of all four methods is very high and comparable. The classification accuracy of all four methods decreases with increasing noise level. However, the classification accuracy of PBSNLR, ReSuMe and MemPo-Learn without the robustness strategy decreases more sharply than the robust MemPo-Learn. The computational model trained by the robust MemPo-Learn rule can maintain a high classification accuracy ($\sim 90\%$) even when the voltage noise reaches a considerably high level (~ 0.4 mV).

2) *Sound Event Classification*: In this section, we carry out experiments to show the performance of our proposed learning method on a sound recognition task. A total of 10 sounds are selected from the Real World Computing Partnership (RWCP) [57] Sound Scene Database in Real Acoustic Environments. The selected categories cover a wide range of sound events, including horn, bells5, bottle1, buzzer, cymbals, kara, metal15, phone4, whistle1 and whistle3. For each event, 40 files are randomly selected as training samples and another 40 files are selected for testing samples. Therefore, the total number of training samples and testing samples are both 400. After training, the average classification accuracy for each method is reported in clean and at 20, 10 and 0 dB signal-to-noise ratio (SNR) for the “Speech Babble” noise environment, taken from the NOISEX’92 database [58].

The encoding method proposed in [59] is used to convert the sound events into spatiotemporal spike patterns. According to the encoding method, the sound is converted from its original domain to a representation in the frequency domain by Fast Fourier Transform (FFT) over several windows. Then, a one-

dimensional order filter is used in the feature extraction stage to select the local maximum in the power spectrum as a **keypoint**, followed by the temporal coding scheme to produce the output spatiotemporal spike patterns. Fig. 20 demonstrates an encoding result of a bottle sound in both clean and 10dB noise. It can be seen that the encoded spatiotemporal spike patterns of clean and noise patterns are very similar. While there are some random spikes in Fig. 20(d) due to the noise, the important information is still represented, therefore the temporal coding method used here is robust. (For more details about the coding method, please see reference [59].)

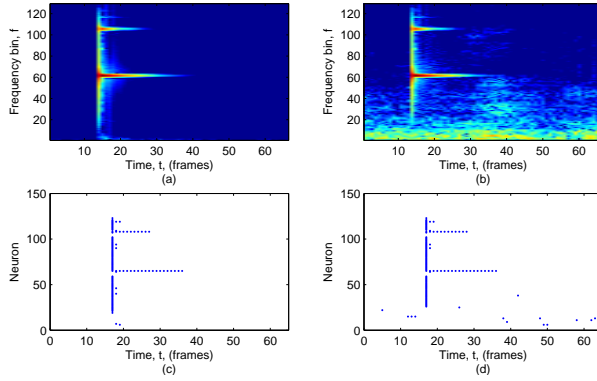


Fig. 20. Examples of encoded spatiotemporal spike patterns. (a) and (b) show the bottle sound in clean and 10 dB noise condition, with the corresponding encoded spike trains shown below.

The learning part of the spiking neural network is composed of one layer of 10 spiking neurons, with each learning neuron corresponding to one category. Each neuron is trained to fire a spike when a corresponding pattern is present, and the desired firing time is when the postsynaptic membrane potential reaches its maximum value. When other patterns are presented, the membrane potential of the learning neuron is trained to below the firing threshold.

In the recognition part, the input pattern will be decided by one of the neurons that generates the most similar spike to the desired spike time. In addition, if all learning neurons remain silent, the learning neuron with the strongest activation state represents the class association. Table. V shows the sound event classification performance of different methods.

TABLE V
CLASSIFICATION ACCURACY OF DIFFERENT METHODS FOR THE SOUND EVENT TASK

Methods	Clean	20dB	10dB	0dB	Average
R-MemPo-Learn	97.8%	97.1%	96.4%	91.1%	95.6%
MemPo-Learn	97.1%	96.2%	95.2%	88.7%	94.3%
PBSNLR	96.9%	96.3%	95.8%	87.2%	94.0%
ReSuMe	95.3%	92.3%	90.3%	85.2%	90.7%
DNN-5 layers	97.5%	97.2%	87.5%	20.2%	75.6%
CNN-5 layers	98.7%	97.3%	91.52%	38.5%	81.5%
CNN-7 layers	97.2%	95.2%	92.7%	25.7%	77.7%

The experimental results are presented in Table. V. It can be seen that the proposed robust MemPo-Learn method performs well for each of the noise conditions, achieving an average accuracy of 95.6%. It can also maintain an accuracy of over 91% in the challenging 0dB SNR condition. The results also

show that the classification accuracy of CNN and DNN is high under clean and low-noise environment, while the performance decreases dramatically with the increase of the noise level. For example, the CNN-5 model can achieve a classification accuracy of 98.7% under clean condition, while the accuracy decreases to 38.5% under the 0dB SNR condition. Therefore, the robustness of the proposed method is better than the traditional neural networks.

VI. DISCUSSION AND CONCLUSION

Analysis of the experiments revealed that the learning performance of MemPo-Learn is much better than that of ReSuMe in terms the learning accuracy and efficiency. The difference in the learning performance between MemPo-Learn and ReSuMe is due to the difference in the training mechanisms. MemPo-Learn is a membrane potential driven method, using the postsynaptic membrane potential rather than postsynaptic spike times as the relevant signal for synaptic changes. In this way, the adjustment of synaptic weights is direct, and it will decrease the difficulty and complexity of the training process. In addition, compared to PBSNLR, MemPo-Learn has **obvious** advantage in terms of learning efficiency. The main reason for this conclusion is that MemPo-Learn is based on gradient descent, and the size of the weight changes is determined by learning rate and the difference between the desired and the actual membrane potential. However, the adjustment of PBSNLR just relates to learning rate. Therefore, MemPo-Learn has higher flexibility and better efficiency.

A small time step can be much closer to continuous time, and is extremely important for real-time applications of SNNs. However, a small time step learning is more difficult and time-consuming. SSTS is proposed to improve the efficiency of a small time step learning. SSTS divides one learning epoch into many sub-epochs, in each sub-epoch, SSTS consists of two main operations: 1) all desired output times are added into monitor time points to resolve inadequate learning for t_d ; 2) jumping to monitor the membrane potential in each sub-epoch to resolve over-adjustment at N_{td} . By using SSTS, we not only overcome over-adjustment and inadequate learning for t_d , but also improve the learning efficiency significantly.

In future work, we will explore how to extend MemPo-Learn to multiple layer networks (three or more layers). It is expected that such an approach would improve the application range and memory capacity of spiking neurons. Another interesting future direction is to search for efficient and biological plausible input and output encoding methods for multiple spikes that can further improve the application performance. Another interesting idea to pursue in the future is to look at how possibly can information-theory be used to derive novel analytic measures of performance and predict network performance based on the quality of input.

APPENDIX EXPERIMENTAL DETAILS.

Unless otherwise stated, our experiments run on MATLAB 7.12.0 on a quad-core system with 16-GB RAM in Windows environment. All parameters of our algorithm are empirical

values. For traditional algorithms, the parameter value scopes provided by their corresponding references are employed in our simulations, and many different values in these scopes are tested to find the one achieving the highest accuracy. During the learning process, MemPo-Learn uses the storage space in exchange for substantial savings in calculation time. All the PSPs induced by every synapse at different time steps need to be calculated and stored before training. Unless the learning neuron can output the target output spikes precisely, the experiments will stop at the upper limit of 1000 learning epoch. In all of the experiments, the value of the neuron model is set as: $\vartheta = 1$ mV, $\lambda = 2$, $\tau = 7$ ms and $\tau_R = 5$ ms.

The experiments of CNN and DNN are run on Python 3.6.1 with TensorFlow 1.3.0 on a quad-core system with 16-GB RAM in Windows environment, and the CNN and DNN are trained on spectrogram using Short-Time Fourier Transform (STFT). The STFT is performed with 50 filters and a 16kHz sampling frequency. The audio signal is down-sampling into 50 frames with 50% overlap. The DNN constructure consists of five fully connected layers with the size set as 1024-512-256-64-10. The CNN-5 model consists of one convolutional layer (8 feature maps with a size of 3×3 filter), one pooling layer (with a 2×2 pooling window), followed by three fully connected layers. The CNN-7 model consists of 2 convolutional layers with $8 \times 3 \times 3$ kernels and $8 \times 2 \times 2$ kernels, respectively. Each convolutional layer is followed by a pooling layer with the same subsample window of 2×2 . Similar to the CNN-5 model, the CNN-7 model is equipped with three fully connected layers.

REFERENCES

- [1] A. Mohemmed, S. Schliebs, S. Matsuda, and N. Kasabov, "Training spiking neural networks to associate spatio-temporal input/output spike patterns". *Neurocomputing*, vol. 107, pp. 3-10, May 2013.
- [2] P. A. Cariani, "Temporal codes and computations for sensory representation and scene analysis". *IEEE Trans. Neural Netw.*, vol. 15, no. 5, pp. 1100-1111, Sep. 2004.
- [3] J. J. Hopfield, "Pattern recognition computation using action potential timing for stimulus representation". *Nature*, vol. 376, no. 6535, pp. 33-36, 1995.
- [4] J. Gautrais and S. Thorpe, "Rate coding versus temporal order coding: A theoretical approach". *BioSystems*, vol. 48, no. 1-3, pp. 57-65, 1998.
- [5] M. J. Berry and M. Meister, "Refractoriness and neural precision". *J. Neurosci.*, vol. 18, no. 6, pp. 2200-2211, Mar. 1998.
- [6] V. J. Uzzell and E. J. Chichilnisky, "Precision of spike trains in primate retinal ganglion cells". *J. Neurophysiol.*, vol. 92, no. 2, pp. 780-789, Aug. 2004.
- [7] T. Gollisch and M. Meister, "Rapid neural coding in the retina with relative spike latencies". *Science*, vol. 319, no. 5866, pp. 1108-1111, 2008.
- [8] P. Reinagel and R. C. Reid, "Temporal coding of visual information in the thalamus". *J. Neuroscience*, vol. 20, no. 14, pp. 5392-5400, Jul. 2000.
- [9] W. Bair and C. Koch, "Temporal precision of spike trains in extrastriate cortex of the behaving macaque monkey". *Neural Comput.*, vol. 8, no. 6, pp. 1185-1202, Aug. 1996.
- [10] W. Wang, B. Subagdjia, A.-H. Tan and J. A. Starzyk, "Neural Modeling of Episodic Memory: Encoding, Retrieval, and Forgetting". *IEEE Trans. Neural Netw. Learn. Syst.*, vol. 23, no. 10, pp. 1574-1586, 2012.
- [11] V. A. Nguyen, J. A. Starzyk, W. B. Goh and D. Jachyra, "Neural Network Structure for Spatio-Temporal Long-Term Memory". *IEEE Trans. Neural Netw. Learn. Syst.*, vol. 23, no. 6, pp. 971-983, 2012.
- [12] W. Gerstner and W. M. Kistler, "Spiking Neuron Models: Single Neurons, Populations, Plasticity". 1st ed. U.K. Cambridge University Press, Aug. 2002.
- [13] S. Ghosh-Dastidar and H. Adeli, "Spiking neural networks". *International journal of neural systems*, vol. 19, no. 4, pp. 295-308, 2009.
- [14] W. Maass, "Networks of spiking neurons: the third generation of neural network models". *Neural networks*, vol. 10, no. 9, pp. 1659-1671, 2006.
- [15] W. Maass, "Fast sigmoidal networks via spiking neurons". *Neural Comput.*, vol. 9, no. 2, pp. 279-304, 1997.
- [16] W. Maass, "Noisy spiking neurons with temporal coding have more computational power than sigmoidal neurons". <http://www.igi.tugraz.at/psfiles/90.pdf>.
- [17] R. Kempter, W. Gerstner and J. L. Van Hemmen, "Spike-based compared to rate-based Hebbian learning". *Advances in neural information processing systems*, vol. 11, pp. 125-131, 1999.
- [18] A. Borst, and F. E. Theunissen, "Information theory and neural coding". *Nature neuroscience*, vol. 2, no. 11, pp. 947-957, 1999.
- [19] E. I. Knudsen, "Supervised learning in the brain". *J. Neuroscience*, vol. 14, no. 7, pp. 3985-3997, 1994.
- [20] H. Qu, X. Xie, et al. "Improved perception-based spiking neuron learning rule for real-time user authentication". *Neurocomputing*, vol. 151, pp. 310-318, 2015.
- [21] W. T. Thach, "On the specific role of the cerebellum in motor learning and cognition: Clues from PET activation and lesion studies in man". *Behavioral Brain Sci.*, vol. 19, no. 3, pp. 411-431, 1996.
- [22] M. Ito, "Mechanisms of motor learning in the cerebellum". *Brain Res.*, vol. 886, no. 1-2, pp. 237-245, Dec. 2000.
- [23] F. Ponulak, and A. Kasinski, "Supervised learning in spiking neural networks with ReSuMe: Sequence learning, classification, and spike shifting". *Neural Comput.*, vol. 22, no. 2, pp. 467-510, 2010.
- [24] A. Taherkhani, A. Belatreche, Y. Li, and L. P. Maguire, "DL-ReSuMe: A Delay Learning-Based Remote Supervised Method for Spiking Neurons". *IEEE Trans. Neural Netw. Learn. Syst.*, vol. 26, no. 12, pp. 3137-3149, Dec. 2015.
- [25] S. M. Bohte, J. N. Kok, and H. La Poutre, "Error-backpropagation in temporally encoded networks of spiking neurons". *Neurocomputing*, vol. 48, no. 1, pp. 17-37, 2002.
- [26] Y. Xu, X. Zeng, L. Han and J. Yang, "A supervised multi-spike learning algorithm based on gradient descent for spiking neural networks". *Neural Networks*, vol. 43, pp. 99-113, 2013.
- [27] R. V. Florian, "The chronotron: a neuron that learns to fire temporally precise spike patterns". *PloS one*, vol. 7, no. 8, e40233, 2013.
- [28] A. Mohemmed, S. Schliebs, S. Matsuda and N. Kasabov, "Span: Spike pattern association neuron for learning spatio-temporal spike patterns". *International journal of neural systems*, vol. 22, no. 4, 2012.
- [29] J. D. Victor and K. P. Purpura, "Metric-space analysis of spike trains: theory, algorithms and application". *Network: computation in neural systems*, vol. 8, no. 2, pp. 127-164, 1997.
- [30] M. Rossum, "A novel spike distance". *Neural Comput.*, vol. 13, no. 4, pp. 751-763, 2001.
- [31] R. Güttig and H. Sompolinsky, "The tempotron: A neuron that learns spike timing-based decisions". *Nature Neuroscience*, vol. 9, no. 3, pp. 420-428, Feb. 2006.
- [32] Y. Xu, X. Zeng and S. Zhong, "A new supervised learning algorithm for spiking neurons". *Neural Comput.*, vol. 25, no. 6, pp. 1472-1511, 2013.
- [33] R. M. Memmesheimer, R. Rubin, B. P. Ölveczky, and H. Sompolinsky. "Learning precisely timed spikes". *Neuron*, vol. 82, no. 4, pp. 925-938, 2014.
- [34] M. Zhang, H. Qu, A. Belatreche and X. Xie. "EMPD: An Efficient Membrane Potential Driven Supervised Learning Algorithm for Spiking Neurons". *IEEE Transactions on Cognitive and Developmental Systems*, DOI: 10.1109/TCDS.2017.2651943, 2017.
- [35] R. Güttig, "Spiking neurons can discover predictive features by aggregate-label learning". *Science*, vol. 351, no. 6277, 2016.
- [36] C. Albers, M. Westkott and K. Pawelzik, "Learning of Precise Spike Times with Homeostatic Membrane Potential Dependent Synaptic Plasticity". *PloS one*, vol. 11, no. 2, e0148948, 2016.
- [37] A. Zador, "Spikes: Exploring the Neural Code". *Science*, vol. 277, no. 5327, pp. 772-773, 1997.
- [38] E. Schneidman, "Noise and information in neural codes". Unpublished doctoral dissertation, Hebrew University.
- [39] M. C. van Rossum, B. J. O'Brien, and R. G. Smith, "Effects of noise on the spike timing precision of retinal ganglion cells". *Journal of Neurophysiology*, vol. 89, pp. 2406-2419, 2003.
- [40] A. L. Hodgkin and A. F. Huxley, "A quantitative description of membrane current and its application to conduction and excitation in nerve". *J. Physiol.*, vol. 117, no. 4, pp. 500-544, 1952.
- [41] E. M. Izhikevich, "Simple model of spiking neurons". *IEEE Trans. Neural Netw.*, vol. 14, no. 6, pp. 1569-1572, 2003.

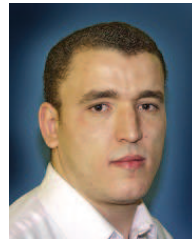
- [42] S. Schreiber, J. M. Fellous, D. Whitmer, P. Tiesinga and T. J. Sejnowski, "A new correlation-based measure of spike timing reliability". *Neurocomputing*, vol. 52, pp. 925-931, 2003.
- [43] F. Ponulak "Analysis of the resume learning process for spiking neural networks". *Appl. Math. Comput. Sci.*, vol. 18, no. 2, pp. 117-127, 2008
- [44] A. Kasiski and F. Ponulak, "Comparison of supervised learning methods for spike time coding in spiking neural networks". *Int. J. Appl. Math. Comput. Sci.*, vol. 16, no. 1, pp. 101-113, 2006.
- [45] J. A. Wall, L. McDaid, L. P. Maguire and T. M. McGinnity, "Spiking Neural Network Model of Sound Localization Using the Interaural Intensity Difference". *IEEE Trans. Neural Netw. Learn. Syst.*, vol. 23, no. 4, pp. 574-586, 2012.
- [46] Q. Yu, H. Tang, K. C. Tan, and H. Li, "Rapid feedforward computation by temporal encoding and learning with spiking neurons". *IEEE Trans. Neural Netw. Learn. Syst.*, vol. 24, no. 10, pp. 1539-1552, 2013.
- [47] B. Zhao, R. Ding, S. Chen, B. Linares-Barranco, and H. Tang, "Feedforward Categorization on AER Motion Events Using Cortex-Like Features in a Spiking Neural Network". *IEEE Trans. Neural Netw. Learn. Syst.*, vol. 26, no. 9, pp. 1963-1978, 2015.
- [48] H. Qu, S. X. Yang, et al., "Real-Time Robot Path Planning Based on a Modified Pulse-Coupled Neural Network Model". *IEEE Transactions on Neural Networks*, vol. 20, no. 11, pp. 1724-1739, 2009.
- [49] C. D. Brody and J. J. Hopfield, "Simple networks for spike-timing-based computation, with application to olfactory processing". *Neuron*, vol. 37, pp. 843-852, 2003.
- [50] J. Hu, H. Tang, K. C. Tan, H. Li, and L. Shi, "A spike-timing-based integrated model for pattern recognition". *Neural Comput.*, vol. 25, no. 2, pp. 450-472, 2013.
- [51] M. Zhang, H. Qu, X. Xie and J. Kurths. "Supervised learning in spiking neural networks with noise-threshold". *Neurocomputing*, vol. 219, pp. 333-349, 2017.
- [52] J. Hu, H. Tang, K. C. Tan and H. Li, "How the Brain Formulates Memory: A Spatio-Temporal Model". *IEEE Computational Intelligence Magazine*, vol. 11, no. 2, pp. 56-68, May 2016.
- [53] H. Qu, Z. Yi and S. X. Yang "Efficient shortest-path-tree computation in network routing based on pulse-coupled neural networks". *IEEE Trans. Cybern.*, vol. 43, no. 3, pp. 995-1010, 2013.
- [54] Q. Yu, H. Tang, K. C. Tan and H. Li, "Precise-Spike-Driven Synaptic Plasticity: Learning Hetero-Association of Spatiotemporal Spike Patterns". *PLoS one*, vol. 8, no. 11, e78318, 2013.
- [55] Q. Yu, R. Yan, H. Tang, et al, "A Spiking Neural Network System for Robust Sequence Recognition". *IEEE Trans. Neural Netw. Learn. Syst.*, vol. 27, no. 3, pp. 621-635, 2016.
- [56] J. Wang, A. Belatreche, L. P. Maguire and T. M. McGinnity, "SpikeTemp: An Enhanced Rank-Order-Based Learning Approach for Spiking Neural Networks With Adaptive Structure". *IEEE Trans. Neural Netw. Learn. Syst.*, vol. 28, no. 1 pp. 30-43, 2017.
- [57] Real World Computing Partnership, "RWCP Sound Scene Database in Real Acoustic Environments," [Online]. Available: <http://tosa.mri.co.jp/sounddb/indexe.htm>.
- [58] A. Varga and H. J. M. Steeneken, "Assessment for automatic speech recognition: Ii. noisx-92: A database and an experiment to study the effect of additive noise on speech recognition systems," *Speech Communication*, vol. 12, no. 3, pp. 247-251, 1993.
- [59] R. Xiao, R. Yan, H. Tang and K. C. Tan, "A Spiking Neural Network Model for Sound Recognition," in *Int. Conf. on Cognitive Systems and Signal Processing*, pp. 584-594, 2016.



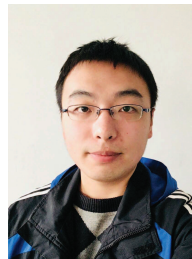
Malu Zhang is a current Ph.D. student in Department of computer science and engineering, University of Electronic Science and Technology of China. His current research interests relate to neural networks, intelligent computation, deep learning and optimization.



Hong Qu received the Ph.D. degree in computer science from the University of Electronic Science and Technology of China, Chengdu, in 2006. From 2007 to 2008, he was a Postdoctoral Fellow at the Advanced Robotics and Intelligent Systems Lab, School of Engineering, University of Guelph, Guelph, ON, Canada. From 2014 to 2015, he worked as a visiting scholar in the Potsdam Institute for Climate Impact Research (PIK), 14473 Potsdam, Germany, and in Humboldt University of Berlin. Currently, he is a professor in Computational Intelligence Laboratory, School of Computer Science and Engineering, University of Electronic Science and Technology of China. His research interests include Neural Networks, Machine Learning and Big Data.



Ammar Belatreche received the Ph.D. degree in computer science from Ulster University, UK. He is currently a Senior Lecturer in computer science at the Department of Computer and Information Sciences, Northumbria University, UK. He previously worked as Lecturer in computer science at the School of Computing and Intelligent Systems, Ulster University, UK. His current research interests include bioinspired adaptive systems, machine learning, pattern recognition, data analytics, capital market engineering, image processing and understanding. Dr. Belatreche is a fellow of the Higher Education Academy, an Associate Editor of *Neurocomputing* and has served as a Program Committee Member and a reviewer for several international conferences and journals.



Chen Yi is a current Ph.D. student in Department of computer science and engineering, University of Electronic Science and Technology of China. His current research interests relate to neural networks, intelligent computation, deep learning and optimization.



Zhang Yi received the Ph.D. degree in mathematics from the Institute of Mathematics, The Chinese Academy of Science, Beijing, China, in 1994. Currently, he is a Professor at the Machine Intelligence Laboratory, College of Computer Science, Sichuan University, Chengdu, China. He is the co-author of three books: *Convergence Analysis of Recurrent Neural Networks* (Kluwer Academic Publishers, 2004), *Neural Networks: Computational Models and Applications* (Springer, 2007), and *Subspace Learning of Neural Networks* (CRC Press, 2010). He was an Associate Editor of *IEEE Transactions on Neural Networks and Learning Systems* (2009–2012), and He is an Associate Editor of *IEEE Transactions on Cybernetics* (2014–). His current research interests include Neural Networks and Big Data. He is a fellow of IEEE.